RESEARCH PAPER

Development and physicochemical characterisation of a cremophor-free paclitaxel–calix[6]arene inclusion complex with increased apparent solubility and in vitro cytotoxicity in mia-pa-ca-2 pancreatic cancer cells

***Bina Gidwani*[1], *Jyoti Sahu* [2, 3*], *Sanjay Kumar Gupta*[4]**

[1] *Columbia Institute of Pharmacy, Faculty of Pharmacy, Columbia Professional University, Raipur, Chhattisgarh, India*
[2] *Shri Rawatpura Sarkar Institute of Pharmacy, Durg, Chhattisgarh, India*
[3] *Vishwakarma University, School of Pharmacy, Pune, Chhattisgarh, India*
[4] *Department of Pharmacology, Rungta College of Pharmaceutical Sciences and Research, Rungta International Skills University, Bhilai, Durg, Chhattisgarh, India*

ABSTRACT

***Objective(s)*:** The current research focused on the development of a Cremophor-free Paclitaxel (PTX)–Calix[6]arene (C6A) inclusion complex. To determine its apparent aqueous solubility and in vitro cytotoxicity against MIA-Pa-Ca-2 pancreatic cancer cells.

***Materials and Methods*:** An optimised PTX–C6A inclusion complex (3:5 mole ratio) was synthesised through physical mixing, and the drug loading was estimated using a validated HPLC technique. The physical characterisation of the inclusion complex was performed using FTIR, DSC, XRD, FESEM, and EDX techniques. The aqueous solubility of the complexes was comparatively studied at pH 6.8 and 7.4 using the UV-visible spectrophotometer technique, and their cytotoxicity in vitro against the MIA-Pa-Ca-2 cell line was evaluated.

***Results*:** The optimised 3:5 inclusion complex (IC) showed 84.7 ± 0.2 % (n=3) drug content, which was calculated using the HPLC technique. The inclusion complex exhibited higher apparent aqueous solubility than free PTX at both pH 6.8 and 7.4, with a more pronounced enhancement at pH 6.8. XRD analysis suggested partial amorphisation of the inclusion complex, while FESEM examination revealed predominantly spherical particles with diameters ranging from approximately 45–60 nm. The FTIR spectra showed no significant variation in the characteristic absorption bands after 12 weeks of storage, indicating no detectable changes in the characteristic FTIR profile during storage. In addition, the inclusion complex showed in vitro cytotoxic activity against MIA-Pa-Ca-2 cells with an IC_{50} of 5.641 nM, which was better than that of PTX (6.705 nM) and C6A (9.450 µM).

***Conclusion*:** The apparent aqueous solubility of the PTX–C6A inclusion complex was slightly higher than that of PTX, accompanied by partial amorphisation of PTX. It also showed higher in vitro cytotoxic activity against MIA-Pa-Ca-2 cells as compared to free PTX. The overall anticancer activity of the inclusion complex could be affected by the intrinsic cytotoxicity of Calix[6]arene; however, further investigation is needed to confirm this contribution.

***Keywords*:** *Calix[6]arene; Cremophor–free formulation; Paclitaxel; Pancreatic cancer; Supramolecular chemistry*

How to cite this article

Gidwani B, Sahu J, Gupta SK. Development and physicochemical characterisation of a cremophor-free paclitaxel–calix[6]arene inclusion complex with increased apparent solubility and in vitro cytotoxicity in mia-pa-ca-2 pancreatic cancer cells. Nanomed J. 2026; 13: 1-. DOI: 10.22038/nmj.2026.83642.2378

Graphical Abstract

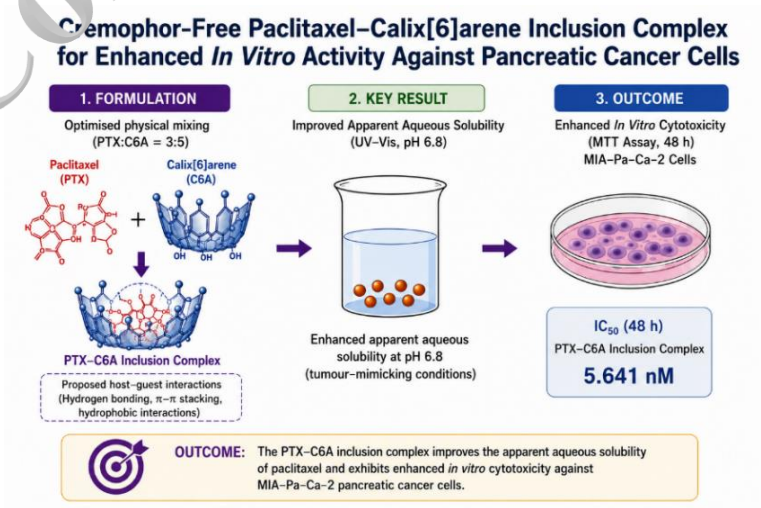

* *Corresponding author(s):* Jyoti Sahu, Assistant Professor, Shri Rawatpura Sarkar Institute of Pharmacy, Durg, Chhattisgarh, India; Vishwakarma University, School of Pharmacy, Pune, Chhattisgarh, India. Phone: +7981762182, Email: *jyotisahupharma@gmail.com*.

Note. This manuscript was submitted on December 18, 2025; approved on July 27, 2026.

ABBREVIATIONS

- **ANOVA:** Analysis of Variance
- **ATR-FTIR:** Attenuated Total Reflectance–Fourier-Transform Infrared Spectroscopy
- **BCS :** Biopharmaceutics Classification System
- **C6A :** Calix[6]arene
- **DMEM :** Dulbecco's Modified Eagle Medium
- **DMSO :** Dimethyl Sulfoxide
- **DSC :** Differential Scanning Calorimetry
- **EDS :** Energy-Dispersive X-ray Spectroscopy
- **FBS :** Foetal bovine serum
- **FESEM :** Field Emission Scanning Electron Microscopy
- **HPLC :** High-Performance Liquid Chromatography
- **IC :** Inclusion complex
- **IC_{50} :** Half-Maximal Inhibitory Concentration
- **MTT :** 3-(4,5-Dimethylthiazol-2-yl)-2,5-diphenyltetrazolium Bromide
- **PBS :** Phosphate-Buffered Saline
- **PEG :** Polyethylene Glycol
- **PTX :** Paclitaxel
- **UV-Vis :** Ultraviolet-Visible Spectroscopy
- **XRD :** X-ray Diffraction

INTRODUCTION

Cancer remains a significant global health burden throughout the world and is a major cause of morbidity and mortality. Cancer development and progression rely on complex molecular signalling mechanisms, changes in the tumour microenvironment, and progressive resistance to current therapeutic approaches (1). Pancreatic ductal adenocarcinoma (PDAC) is one of the deadliest cancers, with a rapid rate of progression, limited treatment options, and poor overall prognosis (2). PTX is a widely used chemotherapeutic drug for the treatment of breast, ovarian and pancreatic cancers. The anti-tumour effect of PTX is mainly due to microtubule stabilisation leading to mitotic arrest and ultimately apoptotic cell death. However, Paclitaxel is classified as a BCS Class IV drug, possessing poor solubility in water and limited intestinal absorption, which contribute to its low oral bioavailability. To increase solubility and to administer the drug through the parenteral route, the marketed formulation of Taxol® uses Cremophor EL (polyoxyethylated castor oil) as solubilising agent. The clinical application of Cremophor EL is limited by dose-related toxicity, such as peripheral neuropathy, nephrotoxicity, and hypersensitivity reactions, which require corticosteroid and antihistamine pretreatment before the administration of Cremophor EL. Therefore, developing a Cremophor EL-free formulation of Paclitaxel is important to for improving the safety of Paclitaxel therapy (3, 4).

Even though the albumin-bound Paclitaxel (Abraxane®) does not employ Cremophor EL and improves the treatment of pancreatic cancer, its clinical utilisation is limited by its high production costs and complicated formulation. Such limitations have made it imperative to develop a delivery system that is cost-effective, devoid of Cremophor EL and promotes solubility of Paclitaxel in water (5,6). Supramolecular host–guest systems, like calixarenes, cyclodextrins, and similar molecular carriers, have emerged as promising approaches for improving the delivery of poorly water-soluble drugs. In comparison with β-cyclodextrin derivatives, C6A offers a large hydrophobic cavity of 9.8 Å as opposed to 4.7 – 8.0 Å of β-cyclodextrin and pH-sensitive phenolic hydroxyl groups, thereby facilitating interactions with hydrophobic molecules like PTX (7). According to the literature, the formation of a complex between PTX and the C6A cavity is thought to be stabilised by hydrophobic interactions, π–π stacking, and hydrogen bonds. Previously, it has been shown that complexation with calixarenes can significantly improve the apparent aqueous solubility of hydrophobic drug molecules. However, the degree of improvement depends on the physicochemical properties of the drug, the type of calixarene derivative used, and the experimental conditions used to prepare and test the complexes. Moreover, the thermal stability of C6A is excellent (decomposition temperature >300 °C), and its solid-state stability exceeds 2 years (8). In addition, calixarene derivatives have been shown to possess intrinsic antiproliferative activity, and their host–guest interactions can potentially improve drug delivery (9). Because of the larger hydrophobic cavity that Calix[6]arene possesses compared with traditional β-cyclodextrins, making it potentially suitable host for the bulky PTX molecule (10).

Supramolecular drug delivery has emerged as a promising field demonstrating the potential of calixarenes as host molecules that increase the effectiveness of drugs through host–guest complexation. Some calixarene derivatives have been reported to possess biological activity by themselves (11). Nevertheless, research on Calix[6]arene as a carrier of Paclitaxel is limited, particularly its ability to increase the pH-dependent aqueous solubility and in vitro anticancer activity of PTX. Despite extensive research on cyclodextrins for Paclitaxel delivery, PTX–C6A complexes are rare (12). MIA-Pa-Ca-2 cells were chosen because they are a well-characterised human pancreatic ductal adenocarcinoma cell model with aggressive cancer features and are widely used for evaluating

anticancer agents. Thus, MIA-Pa-Ca-2 cells provide a well-established in vitro model for evaluating the cytotoxic effects of the PTX–C6A inclusion complex. In addition, according to the available literature, the creation of a Cremophor-free PTX–C6A inclusion complex in MIA-Pa-Ca-2 pancreatic cancer cells has not been previously described (Table 1).

Table 1. A comparison and summary of previously reported PTX host-guest delivery systems

Formulation (host; notes)	Solubility (mg/mL or fold-increase; method/conditions)	IC50 / in-vitro test (cell line, units)	Reported drawback/limitation	Ref
Bridged bis (β-CDs) with tetraethylenepentaamino spacer	Up to 2 mg/mL in water (phase-solubility)	K562 leukemia: IC50 = 6.0×10^{-10} mol/dm³ (complex) vs 9.8×10^{-10} mol/dm³ (PTX)	None specified; focus on improved solubility and activity	[13]
Oligo(ethylenediamino)-bridged bis(β-CDs)	Up to 2 mg/mL and 0.9 mg/mL in water	K562: IC50 = 6.0×10^{-10} mol/dm³ (complex) vs 9.8×10^{-10} mol/dm³ (PTX)	None specified	[14]
PTX/DM-β-CD Inclusion complex in Pluronic F127 gel (buccal delivery)	Inclusion complex solution: 0.1 mg/mL PTX released >90 % drug in 3 days in PBS pH 7.4; free PTX showed little release due to poor solubility	KB oral cancer cells: MTT assay showed "acceptable cytotoxicity" vs blank gels (>80 % viability); no numeric IC50 given	No clear drawback; focus on sustained release and buccal system	[15]
PTX/DM-β-CD Inclusion complex in chitosan nanoparticles	"Dramatically enhanced" PTX solubility in water; loading efficiency of NPs was 30.3-fold higher than PTX-loaded CS NPs; no explicit mg/mL value given	Sustained release; pharmacokinetics vs Taxol®, but no IC50 values reported	Hypersensitivity toxicity drawback reported; improved AUC and MRT vs Taxol®	[16]
β-CD derivatives with PTX (various CDs; preformulation study)	Increased aqueous solubility up to 500 times vs Taxol vehicle at ≤5:1 molar ratio CD:PTX	PC-3, A2780, MCF-7, HT-29, A549: ID50 values for complexes lower than free PTX (higher cytotoxicity); exact numbers not given	CDs showed no cytogenotoxicity up to 50 mg/mL; no specific drawbacks listed	[17]
β-CD-g-polyglycerol hybrid nanocarrier with PTX Inclusion complex	Significant enhancement in aqueous solubility of PTX (no numeric value provided)	Not reported in the abstract/full text excerpt provided	None described in the abstract/excerpt provided	[18]
β-CD-poly(N-isopropylacrylamide) star polymer/PTX Inclusion complex (thermoresponsive)	Significantly improved solubilization of PTX by inclusion; no numeric value given in abstract/excerpt provided	A2780/T multidrug-resistant cells: better antitumor effects than commercial PTX; no IC50 given in abstract/excerpt provided	None specified in abstract/excerpt provided	[19]
PTX/DM-β-CD complex in PEGylated liposomes ("double-loaded")	Aqueous solubility increased ~3×10^{10}-fold over pure drug after DM-β-CD complexation (exact baseline not stated); liposomal system size ~163 nm, zeta potential -5.6 mV, drug loading comparable vs standard liposomes	SKOV-3 ovarian cancer cells: IC value improved by 4.2-fold vs Taxol at 48 h; higher cytotoxicity observed but exact IC50 not stated here	Low haemolytic potential for blank liposomes; no major drawback reported in abstract/excerpt provided	[20]
Amphiphilic CD nanoparticles with PTX Inclusion complexes (various charge types)	Inclusion complexes formed; no numeric solubility data given in abstract/excerpt provided	Breast cancer models: stronger antitumor activity than drug solution in both 2D and especially 3D cultures; no IC50 numbers given here	Activity differed between culture models; no specific safety drawbacks reported here	[21]
β-CD Inclusion complex with PTX ("Trojan horse" sugar-cyclodextrin conjugate)	Entrapped hydrophobic PCTX within hydrophilic shell of carbohydrate-cyclodextrin; increased solubility implied but not quantified numerically here	A549 lung cancer cells: internalized via caveolin-1 endocytosis and triggered apoptosis via ROS formation; zebrafish larvae showed lower toxicity compared to PCTX alone; no numeric IC50 given here	None specific—described as more innocuous to non-cancerous cells than free PCTX alone based on zebrafish model data presented here	[22]
β-CD/PTX Inclusion complex for triple-negative breast cancer cells (MDA-MB-231) – optimal ratio found by docking & experiment is β-CD:PTX = 1:2 molar ratio ("IC")	>95 % entrapment efficiency and "improved PTX solubility"; no numeric mg/mL value given here	MDA-MB-231 breast cancer cells: "critical cytotoxicity", decreased colony formation and migration were observed, but no numeric IC50 value was stated	No specific drawback noted	[23]
PTX-Calix[6]arene Inclusion complex (3:5 molar ratio; Cremophor-free supramolecular host-guest system)	UV-visible spectrophotometric analysis showed higher aqueous apparent solubility for the inclusion complex than for free PTX at pH 6.8, indicating an enhanced aqueous solubility.	MIA-Pa-Ca-2 pancreatic cancer cells; MTT assay; IC_{50} = 5.641 nM vs 6.705 nM for free PTX	pH-responsive solubilisation and enhanced cytotoxicity against pancreatic cancer cells	Present study

Notes: Genexol-PM is an approved Cremophor-free micellar PTX (PEG–PLA) injectable; the reported concentration is 6 mg/mL (Park et al., CCR 2004). Citations: See references above; data taken from the stated publications (solubility measured by HPLC or spectrophotometry in water or buffer) and 50 % inhibitory concentration (MTT or similar assays). "Not reported" indicates that the source did not explicitly provide that value (although formulations generally retain PTX's low-nanomolar IC_{50}) (24).

Accordingly, the present study was undertaken to design and characterise a Cremophor-free PTX–C6A inclusion complex and to assess its apparent aqueous solubility and in vitro cytotoxicity against MIA-Pa-Ca-2 pancreatic cancer cells (Figure 1).

MATERIALS AND METHODS

Chemicals and reagents

Paclitaxel (PTX) was received as a gift sample from N.N. Enterprises, Pune. Calix[6]arene was purchased from Tokyo Chemical Industry (Tokyo, Japan). Ethanol, polyethylene glycol (PEG-400), phosphate-buffered saline (PBS), and other analytical-grade reagents were purchased from New Neeta Chemicals (Pune, Maharashtra, India). The human pancreatic ductal adenocarcinoma cell line MIA-Pa-Ca-2 was obtained from the National Centre for Cell Science (NCCS; Pune, India).

Ethical Compliance

All experimental procedures were performed at the School of Pharmacy, Vishwakarma University, Pune, India, in accordance with the institutional laboratory and biosafety guidelines. Institutional Ethics Committee approval was not required for this study, as it involved only authenticated established human cell lines obtained from the NCCS and did not involve any human participants or animal experiments.

Preparation of the Inclusion Complex

PTX–C6A inclusion complexes were prepared at PTX: C6A molar ratios of 1:2, 2:4, and 3:5 using three different preparation techniques: kneading, physical mixing, and solvent evaporation.

Kneading method: C6A was transferred to a mortar and moistened with a small volume of ethanol. PTX in powder form was incorporated and kneaded for 30 min. PEG-400 (1 ml) was added as a stabiliser. The mixture was dried overnight at room temperature (26 ± 2°C) and sieved with a 60-mesh sieve (25).

Physical mixing method: PTX and C6A were dissolved separately in 10 ml of ethanol, and the solutions were maintained at 60 °C during sonication for 15 min using a probe sonicator. The C6A solution was added dropwise to the PTX solution under magnetic stirring (600 rpm for 12 h). PEG-400 (1 mL) was added as a stabiliser. The mixture was centrifuged (10,000 rpm, 15 min, 25 °C), washed once with 5 mL of distilled water, and dried in a desiccator for 24 h (26).

Solvent evaporation technique: PTX and C6A were separately dispersed in 10 mL of ethanol. C6A was sonicated in a probe sonicator, stirred for 30 min at 55 °C, and PTX was added dropwise (600 rpm, stirring for 6 h). PEG-400 (1 mL) was added, and the solvent was evaporated, and the final product was frozen at -80 °C and then lyophilised for 24 h (27).

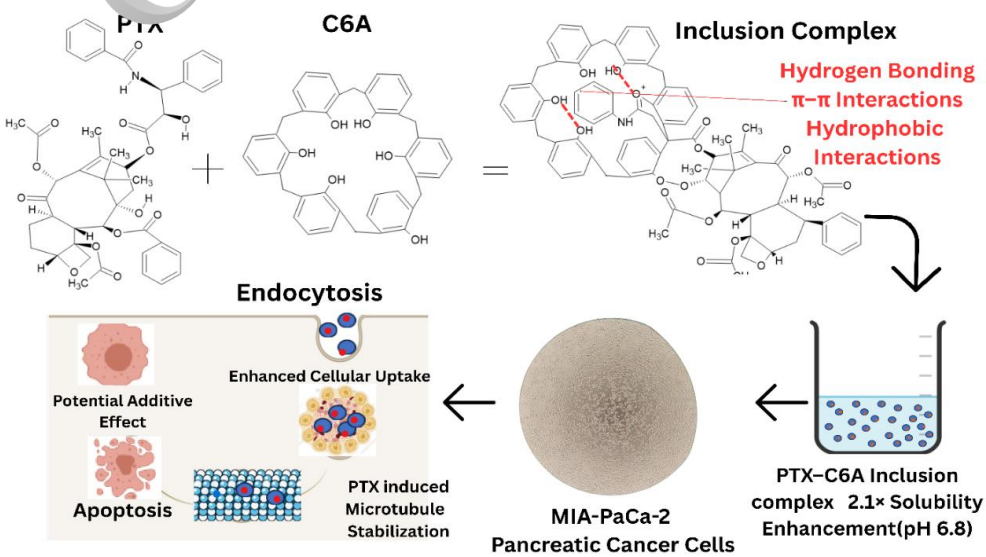

Fig. 1. Schematic illustration of the formation process of the PTX–C6A host-guest inclusion complex. Formation of the complex is hypothesised to take place due to the formation of noncovalent bonds such as hydrogen bonding, π-π stacking, and hydrophobic interactions. This results in increased solubility in water, which increases the accessibility of PTX to the target site and improves its in vitro cytotoxic activity against MIA-Pa-Ca-2 pancreatic cancer cells

The optimised PTX–C6A inclusion complex was prepared separately three times (n = 3) for physicochemical characterisation and further analyses to ensure reproducibility. The formulation showing the highest drug content was selected as the optimised formulation for further physicochemical characterisation and biological evaluation.

Analytical characterisation

The PTX–C6A inclusion complex was extensively characterised using multiple analytical methods to explore its physicochemical properties.

ATR-FTIR spectroscopy

The possible interactions between the functional groups of PTX and C6A were examined using ATR-FTIR spectroscopy. The spectra were collected on a Bruker Alpha-II spectrometer equipped with an ATR crystal between 4000–400 cm -1 with 2 cm -1 resolution at ambient temperature. The shifts in peak positions, changes in band intensity, and peak broadening of the samples were compared with the characteristic absorption bands of PTX and C6A (28).

Differential Scanning Calorimetry (DSC)

DSC was used to investigate the thermal behaviour and physical state of PTX, C6A, and the PTX–C6A inclusion complex. Samples (approximately 2 mg of each sample) were sealed in aluminium pans and heated from 25 to 300 °C at 10 °C/min under nitrogen flow (50 mL/min) using a Mettler Toledo DSC 1. Temperature calibration was performed using indium standards (29).

X-ray Diffraction (XRD)

XRD was used to evaluate the crystallinity and amorphous characteristics of the samples. Patterns were recorded on a Rigaku Miniflex 600 diffractometer (Tokyo, Japan) using Cu Kα radiation (λ = 1.5406 Å) over a 2θ range of 5–50°, step size of 0.02°, and scan speed of 2°/min, at 40 kV and 15 mA (30).

Field Emission Scanning Electron Microscopy (FESEM)

FESEM imaging was used to visualize the particle morphology and size of the PTX–C6A inclusion complex and its individual components. The samples were sputter-coated with gold (~10 nm thickness) to enhance conductivity and imaged using a Nova NanoSEM 450 microscope operating at 15 kV under high vacuum (31).

Energy-Dispersive X-ray Spectroscopy (EDS)

Elemental compositional analyses through EDS were performed to acquire both qualitative and semi-quantitative information about the elemental composition. The distribution of elements such as carbon, oxygen, and nitrogen were evaluated to assess the elemental composition of inclusion complex. Signals from gold coating sputtering were not included in the analysis (15 kV in a high vacuum) (32).

High-Performance Liquid Chromatography (HPLC)

HPLC was used to quantify PTX and calculate the drug content (%) of the PTX–C6A Inclusion complex. The procedure was performed using Shimadzu HPLC equipment under the control of LabSolutions software (C18 analytical column 250 × 4.6 mm, 5 µm). The separation was carried out via isocratic elution with acetonitrile and phosphate buffer (pH 4.5; 65:35, v/v) at a flow rate of 1.5 mL/min. PTX was identified via UV detection at 254 nm with a 20 µL injection volume, and the temperature of the column was kept constant at 25 °C. Prior to analysis, the samples were filtered through a 0.22 µm membrane filter. The PTX concentration was determined from the PTX calibration curve obtained by HPLC, and the drug content (%) of the inclusion complex was calculated using the following equation (33):

Drug Content = Measured Amount of PTX in IC/ Theoretical Amount of PTX in IC *100

Evaluation of apparent aqueous solubility at physiological (pH 7.4) and tumour-mimicking (pH 6.8)

The apparent aqueous solubility of pure PTX and the PTX–C6A inclusion complex was assessed under physiological (pH 7.4) and tumour-mimicking (pH 6.8) conditions using UV–visible spectrophotometry. Pure PTX (10 mg) and a PTX–C6A Inclusion complex containing an equivalent quantity of PTX, as determined from the HPLC-derived drug content, were separately dispersed in 10 mL of phosphate-buffered saline (PBS; pH 6.8 or 7.4). The dispersions were stirred at 50 °C and 600 rpm for 1 h. Following dispersion, each sample was serially diluted with acetonitrile to obtain nominal PTX concentrations of 10, 20, 30, 40, 50, and 60 µg/mL. The solutions obtained were filtered using a 0.45 µm syringe filter, and their absorbance at 254 nm was measured using a UV–visible spectrophotometer. The absorbance of pure PTX and the PTX–C6A inclusion complex were measured at different pH values to determine and compare their apparent aqueous solubility. All experiments were carried out in triplicate, and the data are represented as mean ± SD (n = 3). All data were subjected to statistical analysis using GraphPad Prism software (Version 11.0.2). A two-way analysis of variance (ANOVA) test was applied to assess the

differences among groups, and a p-value < 0.05 was considered statistically significant. There was no absorbance recorded for the blanks containing Calix[6]arene, PEG-400, and PBS at the 254 nm wavelength used for the UV–visible spectrophotometric analysis (34).

Stability studies

To determine stability, the inclusion complex was placed in airtight containers at 4°C for 12 weeks. The physical appearance was visually checked periodically to determine whether there was any colour change, aggregation, or caking. Changes in characteristic functional groups that may indicate degradation or structural changes were determined by measuring the ATR-FTIR spectra at baseline and at the end of 12 weeks (35).

MTT assay

Cell culture

Human pancreatic carcinoma MIA-Pa-Ca-2 cells were cultured in Dulbecco's Modified Eagle Medium (DMEM) supplemented with 10 % foetal bovine serum (FBS), 1 % penicillin-streptomycin, and 2 mM L-glutamine under standard conditions (37°C, 5 % CO_2, humidified atmosphere).

MTT cytotoxicity assay

The cytotoxic effects of the test samples were assessed using the 3-(4,5-dimethylthiazol-2-yl)-2,5-diphenyltetrazolium bromide (MTT) assay. MIA-Pa-Ca-2 cells were seeded in 96-well plates at a density of 8,000 cells per well and allowed to attach overnight under standard cell culture conditions. The cells were then treated with PTX, Calix [6] arene (C6A), and the PTX–C6A inclusion complex (IC) at final concentrations of 0.001, 0.1, 0.25, 0.5, 1, 5, and 10 nM. Untreated cells were used as controls, and each concentration was evaluated in triplicate.

Following a 48-h treatment period, MTT solution (0.5 mg/mL) was added to the cells, which were then incubated at 37 °C for 4 h to generate formazan crystals. The culture medium was removed, and the crystals were dissolved in 150 µL of HPLC-grade dimethyl sulfoxide (DMSO). The plates were left at room temperature for 30 min to ensure complete dissolution before recording the absorbance at 540 nm using a microplate reader. All experimental conditions were tested in triplicate (36).

Data Analysis and IC_{50} Determination

The values of absorbance were normalised to control wells to determine the % cell viability of each sample, which was calculated as follows,

% Cell Viability = (Absorbance treated/Absorbance control) *100

The absorbance and cell-viability data were expressed as mean ± standard deviation (SD) of three replicate wells. Concentration–response data were subjected to nonlinear dose–response regression using the Dose Curve online IC_{50} calculator. IC_{50} values were determined from the fitted concentration–response curves, and the corresponding 95% confidence intervals (CIs), Hill slopes, upper and lower asymptotes, and R^2 values were recorded. A successful convergence of the nonlinear regression model was confirmed for each treatment (37).

RESULTS

Optimisation of PTX–C6A inclusion complex and determination of drug content

Among the three preparation techniques evaluated, physical mixing produced the highest drug content for the PTX–C6A inclusion complex at a PTX: C6A molar ratio of 3:5. The optimised formulation yielded a drug content of 84.7 ± 0.2 %, whereas the drug contents obtained from the solvent evaporation and kneading techniques were 78.25 ± 0.03 % and 50.11 ± 0.11 %, respectively (Table 2). These results indicate that physical mixing produced the highest PTX content under the investigated conditions. Based on the higher drug content achieved with the physical mixing process, this approach was selected as the most suitable for preparing the PTX–C6A inclusion complex. The higher drug content observed at the 3:5 molar ratio may be attributed to the greater availability of Calix[6]arene host cavities, which may facilitate interactions with the bulky PTX molecules. Complete encasement of PTX within a Calix[6]arene unit is not possible, taking into account the size and structure of the PTX molecule. Therefore, partial inclusion along with noncovalent interactions such as hydrophobic interactions, hydrogen bonding, and π–π stacking may have contributed to the stabilisation of the supramolecular complex.

Table 2. Drug content (%) across preparation methods (mean ± SD, n=3)

Drug complex	Methods	Percentage drug content
PTX–C6A inclusion complex	Kneading method	50.11 % ± 0.11 %
	Physical mixing method	84.7 ± 0.2 %
	Solvent evaporation method	78.25 % ± 0.03 %

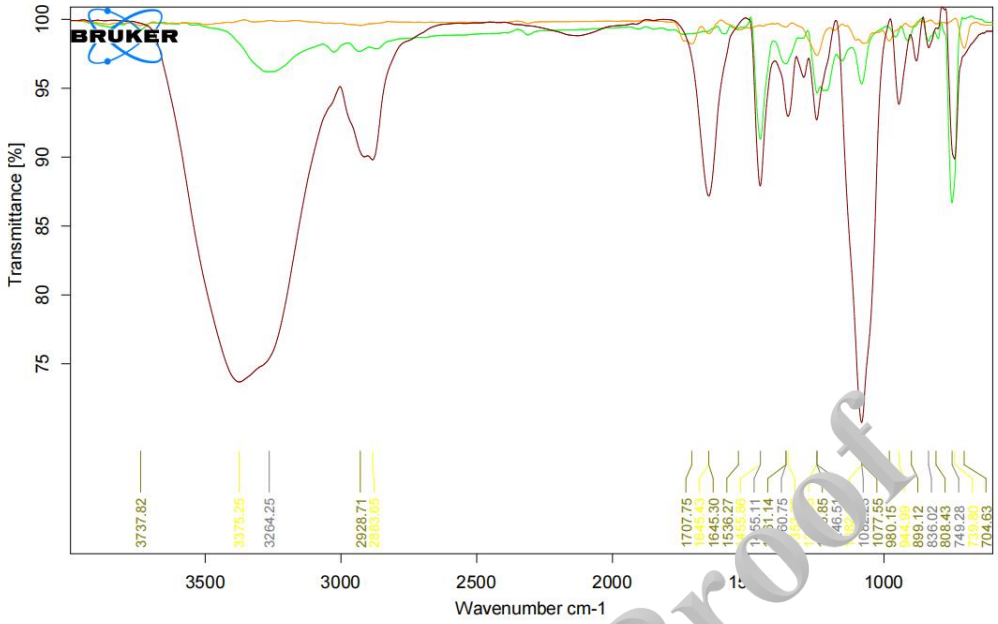

Fig. 2. Comparative FTIR spectra of PTX (green), C6A (orange), and the PTX–C6A inclusion complex (brown) showing changes in the absorbance peak positions and intensities following complexation, indicating hydrogen bonding, π–π stacking, hydrophobic interactions, and partial inclusion of PTX within the Calix[6]arene host structure.

ATR-FTIR analysis

The ATR-FTIR spectra of PTX, C6A, and the PTX–C6A inclusion complex are shown in Figure 2. The absorption peaks of pure PTX appear at around 1730 cm^{-1} (C=O stretching), 1240 cm^{-1} (asymmetric C–O–C stretching) and 3500–3300 cm^{-1} (O–H stretching). After complexation, the carbonyl stretching peak at 1707.75 cm^{-1} shifted to 1715.43 cm^{-1}, while the C–H stretching peak at 2928.71 cm^{-1} shifted to 2838.65 cm^{-1}. Additionally, broadening of the O–H stretching region and slight changes in characteristic absorption peaks of C6A were observed.

The shifts in the peak positions and broadening of the peaks demonstrate the change in the molecular environment of PTX after complexation. This implies that host–guest interactions between PTX and Calix[6]arene occurred. The observed results are indicative of hydrogen bonding, hydrophobic interactions and π–π interactions, suggesting the formation of the PTX–C6A supramolecular inclusion complex. Furthermore, the absence of additional absorption bands implies that complex formation took place through noncovalent interactions and not through the formation of new covalent bonds.

Differential Scanning Calorimetry (DSC)

The DSC thermograms of PTX, C6A, and the PTX–C6A inclusion complex are presented in Figure 3, and the corresponding thermal parameters are summarised in Table 3. PTX exhibited a clear and sharp melting peak at 224.13 °C, confirming the crystalline characteristics of the material. On the other hand, C6A showed a broad thermal transition with a midpoint of 193.37 °C. These findings suggest that C6A crystallises at a lower degree of crystallinity than PTX. In addition, the PTX–C6A inclusion complex showed a faint melting endotherm at 238.22 °C.

The decrease in the intensity of the PTX melting peak and the shift in its peak suggest that PTX changed its physical state after complexation (Table 3).These thermal changes suggest reduced crystallinity and improved molecular dispersion of PTX within the Calix[6]arene matrix. The suppression of the PTX melting transition may be attributed to host–guest interactions between PTX and Calix[6]arene, which interfere with the crystalline organisation of the drug.

Table 3. Thermal parameters of PTX, Calix[6]arene (C6A), and the PTX–C6A Inclusion complex were determined by differential scanning calorimetry (DSC).

Sample	Onset (°C)	Peak (°C)	End set (°C)
PTX	224.77	224.13	243.78
C6A	192.11	193.37*	324.00
PTX–C6A Inclusion complex	237.62	238.22	239.67

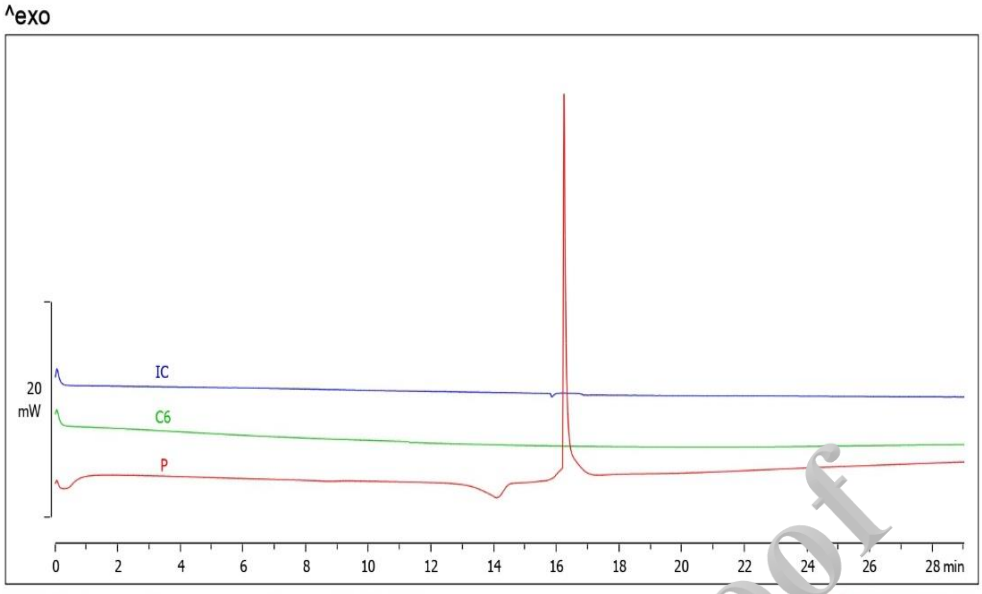

Fig. 3. Overlay of DSC graphs of PTX (P, red), Calix[6]arene (C6, green), and the PTX–C6A inclusion complex (IC, blue). PTX exhibited a distinct endothermic melting peak at approximately 16.2 min, suggesting that the compound was crystalline. C6A exhibited a broad and weak thermal transition, suggesting an amorphous character. On the other hand, the PTX–C6A inclusion complex exhibited a marked reduction in the intensity of the PTX melting endotherm, indicating reduced crystallinity, enhanced molecular dispersion of PTX within the Calix[6]arene matrix, and successful host–guest complex formation.

These observations support the formation of the PTX–C6A inclusion complex and are consistent with the partial amorphisation observed in the XRD analysis.

X-ray Diffraction (XRD)

The XRD diffractograms of PTX, C6A, and the PTX–C6A inclusion complex are presented in Figure 4. Pure PTX exhibited sharp and intense diffraction peaks, confirming its highly crystalline nature. On the contrary, C6A exhibited a broad halo-type pattern, which is typical of an amorphous substance.

The PTX–C6A inclusion complex exhibited a significant decrease in the intensity of the characteristic PTX diffraction peaks, along with the appearance of a broad diffraction pattern, suggesting partial amorphisation of PTX after complex formation.

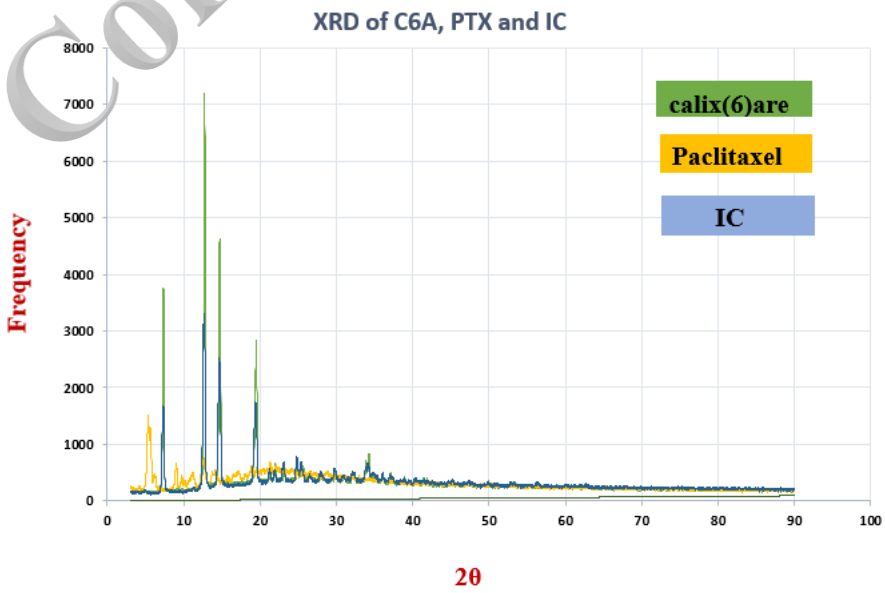

Fig. 4. The peaks of PTX and C6A, along with their PTX–C6A inclusion complex in the XRD diffractograms, have distinct peaks of pure PTX along with reduced peaks in the inclusion complex, indicating a reduction in crystallinity upon complex formation.

The decrease in the intensity of the characteristic PTX diffraction peaks indicates the reduction in crystallinity after complexation with the Calix[6]arene. The decrease in crystallinity was consistent with changes in the physical state of PTX and could be responsible for the increased aqueous solubility of the inclusion complex. This is in accordance with the DSC findings and supports the partial amorphisation of PTX in the PTX–C6A inclusion complex.

Field Emission Scanning Electron Microscopy (FESEM)

Figures 5 and 6 show FESEM images of the PTX, C6A, and PTX–C6A inclusion complexes. While pure PTX showed irregular crystalline particles with sharp edges, C6A demonstrated irregularly aggregated particles with a relatively smooth surface structure. The PTX–C6A inclusion complex appeared as mostly spherical nanoparticles with smooth surfaces. The particle size based on FESEM images revealed that the diameter of the particles was approximately 45–60 nm.

The observed alteration in the particle morphology following complexation is consistent with the changes in the physiochemical characteristics of the formulation. The formation of uniformly distributed spherical particles is consistent with the formation of the PTX–C6A inclusion complex and supports the physicochemical findings obtained from the DSC and XRD analyses.

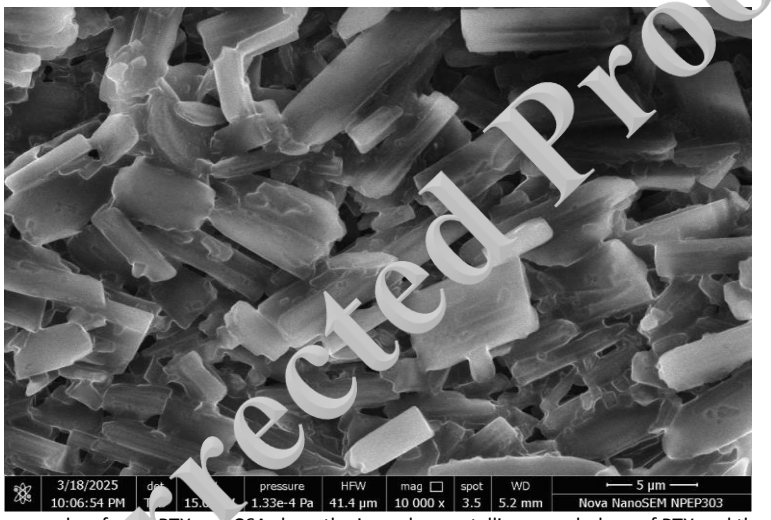

Fig. 5. The FESEM micrographs of pure PTX and C6A show the irregular crystalline morphology of PTX and the aggregation of C6A.

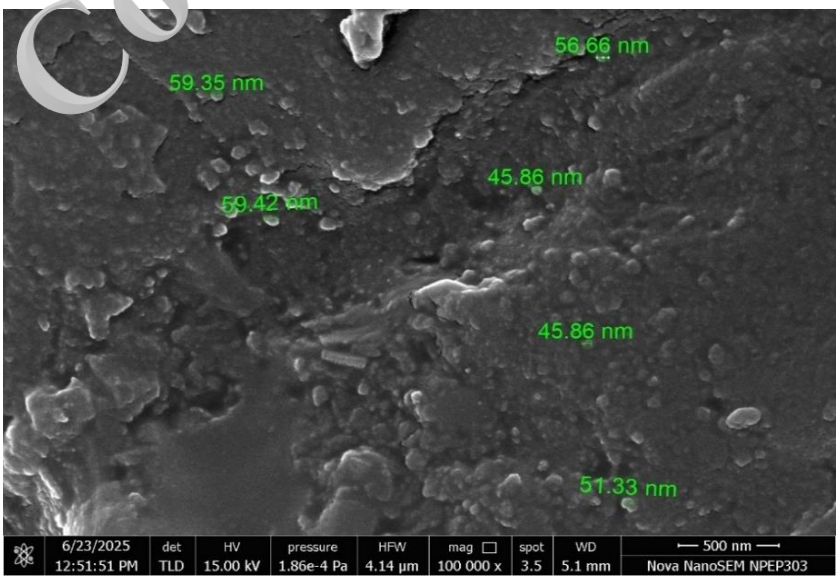

Fig. 6. Representative FESEM micrograph of the PTX–C6A inclusion complex (100,000×; scale bar = 100 nm) showing predominantly spherical nanoparticles with smooth surfaces and particle diameters ranging from approximately 45 to 60 nm.

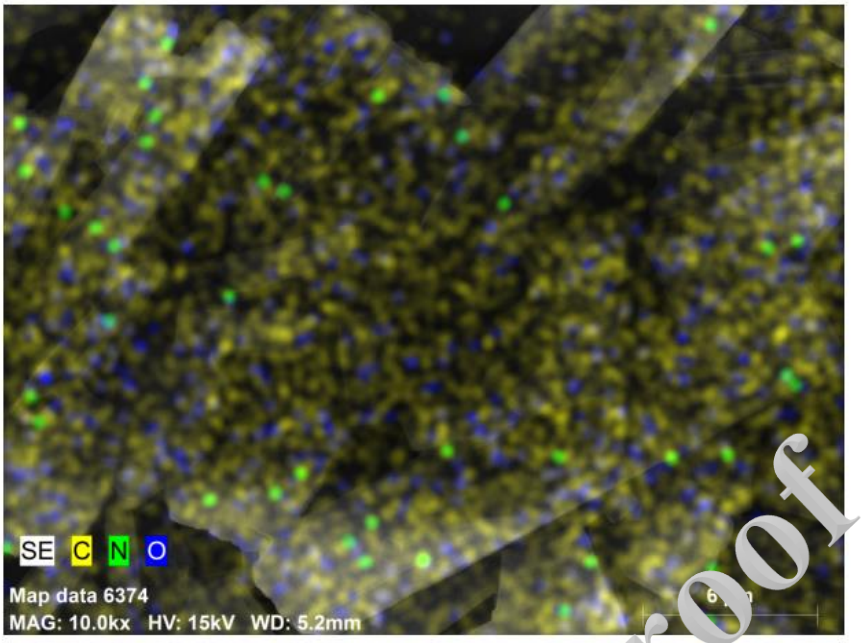

Fig. 7. EDS elemental mapping of the PTX–C6A inclusion complex demonstrated a uniform distribution of carbon, oxygen, and nitrogen within the nanoparticles.

Energy-Dispersive X-ray Spectroscopy (EDS)

Elemental distribution maps obtained by EDS for the PTX–C6A inclusion complex are shown in Figure 7. The distributions of carbon, oxygen, and nitrogen were even throughout the investigated area, suggesting detection of the elemental distribution of the PTX–C6A inclusion complex. No signs of elemental segregation or phase separation were observed.

Although EDS cannot prove the formation of host–guest complexation of PTX and C6A, the even elemental distribution provides indirect evidence of the homogeneous elemental distribution within the formulation. These findings further support the results of the morphological analysis obtained from FESEM.

High-Performance Liquid Chromatography (HPLC)

The chromatograms of the PTX standard, C6A, and PTX–C6A inclusion complex are shown in Figures 8-10. The HPLC calibration curve, constructed from PTX standard concentrations of 10–150 µg/mL, showed good linearity ($y = 50431x + 254567$; $R^2 = 0.9948$), confirming that the method was suitable for PTX quantification over the tested concentration range.

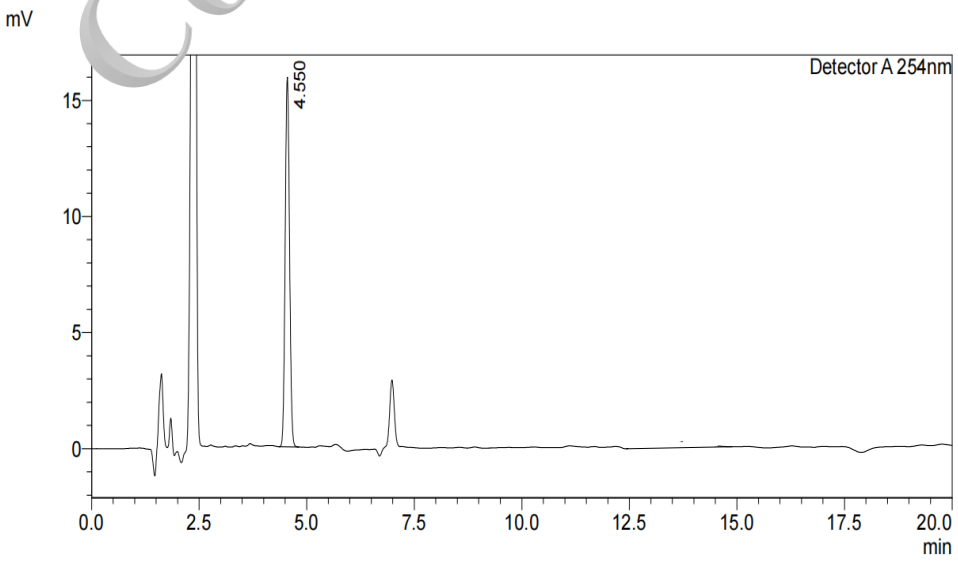

Fig. 8. Representative HPLC chromatogram of the PTX standard showing the characteristic retention peak of PTX.

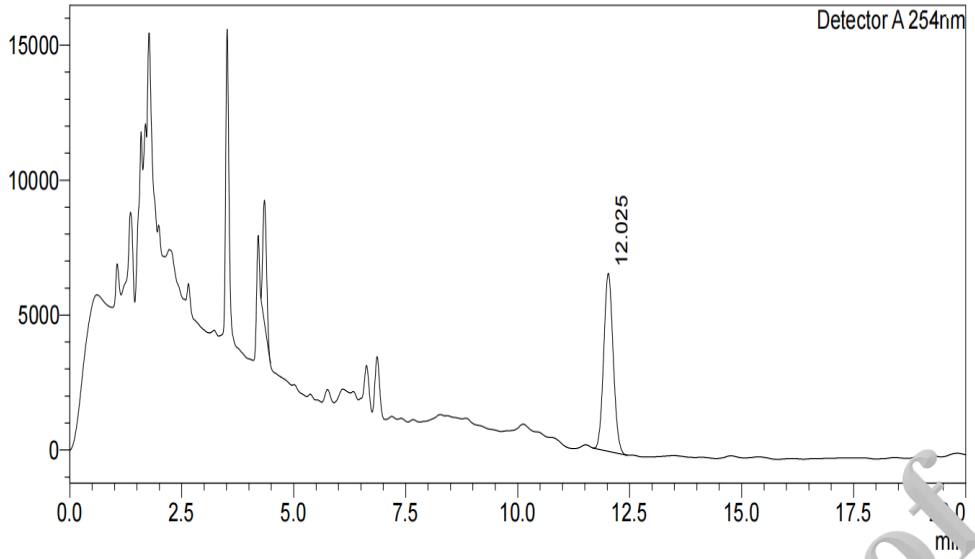

Fig. 9. Representative HPLC chromatogram of the C6A standard

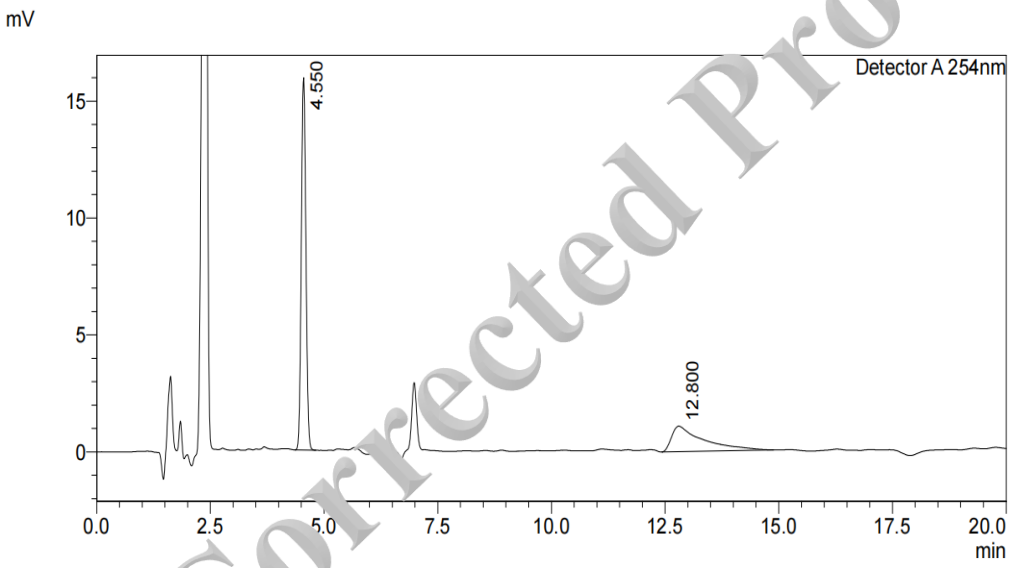

Fig. 10. Representative HPLC chromatograms of standard PTX, calix[6]arene, and the optimised PTX–C6A inclusion complex showed well-resolved chromatographic peaks and the absence of observable interference, enabling the accurate quantification of PTX.

The PTX peak in the chromatogram of the PTX–C6A inclusion complex was sharp and well defined, with no detectable degradation products or impurities, indicating that PTX remained stable throughout the complexation process. Based on the calibration equation (Table 4), the PTX concentration in the optimised inclusion complex was calculated to be 37.76 µg/mL, corresponding to a drug content of 84.7 ± 0.2 % (n = 3). The relatively high drug content reflects effective incorporation of PTX into the optimised PTX–C6A inclusion complex prepared using the physical mixing method. Overall, these findings are consistent with the successful preparation of the optimised PTX–C6A inclusion complex.

Table 4. HPLC analytical parameters and quantitative determination of PTX in the optimised PTX–C6A Inclusion complex.

Parameter	Result
Retention time (PTX)	4.550
Concentration range	10–150 µg/mL
Regression equation	y = 50431x + 254567
R^2	0.9948
PTX concentration	37.76 µg/mL
Drug content	84.7 ± 0.2 %

Apparent aqueous solubility at physiological (pH 7.4) and tumour-mimicking (pH 6.8) conditions

The apparent aqueous solubility of pure PTX and the PTX–C6A inclusion complex was evaluated by comparing their UV absorbance under physiological (pH 7.4) and tumour-mimicking (pH 6.8) conditions. As shown in Figure 11 and Figure 12, the PTX–C6A inclusion complex exhibited higher absorbance than free PTX at both pH values, which suggests greater aqueous solubility due to complexation.

The absorbance increased more markedly at pH 6.8 than at pH 7.4, suggesting greater apparent aqueous solubility of the inclusion complex under slightly acidic conditions. Two-way ANOVA indicated significant differences among the formulations and pH conditions ($p < 0.05$). Thus, the PTX–C6A inclusion complex exhibited greater apparent aqueous solubility under slightly acidic conditions (pH 6.8).

Stability studies

No change in colour and appearance of the PTX–C6A inclusion complex was observed over the 12 weeks storage period at 4 ºC (Figure 13b), and there was no significant change in the characteristic absorption peaks of the complex compared to the spectral data obtained before storage (Figure 13a). The lack of significant changes in the ATR-FTIR spectra suggests that the PTX–C6A inclusion complex maintained good stability during storage.

Based on the favourable physicochemical characteristics and stability of the optimised formulation, its in vitro cytotoxic activity was evaluated against MIA-Pa-Ca-2 pancreatic cancer cells.

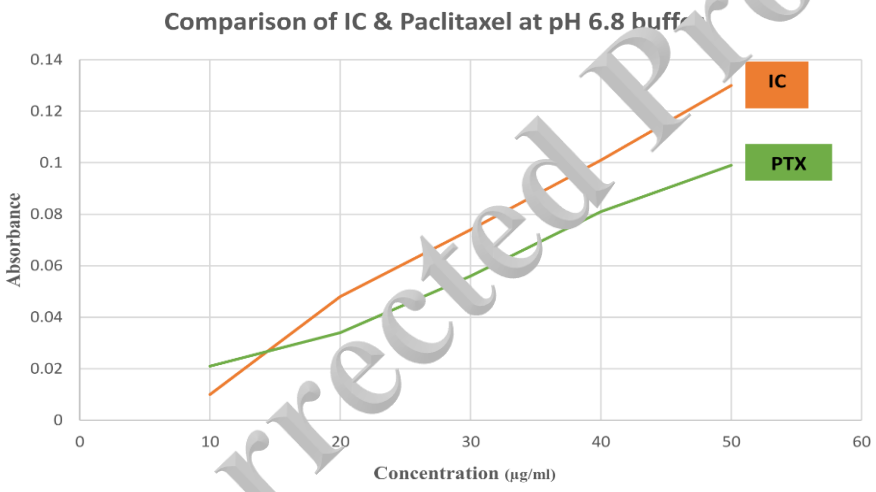

Fig. 11. Apparent aqueous solubility of pure PTX and the PTX–C6A inclusion complex at pH 6.8, determined by UV–visible spectrophotometry. Data are presented as mean ± SD (n = 3). Statistical significance was evaluated using two-way analysis of variance (ANOVA).

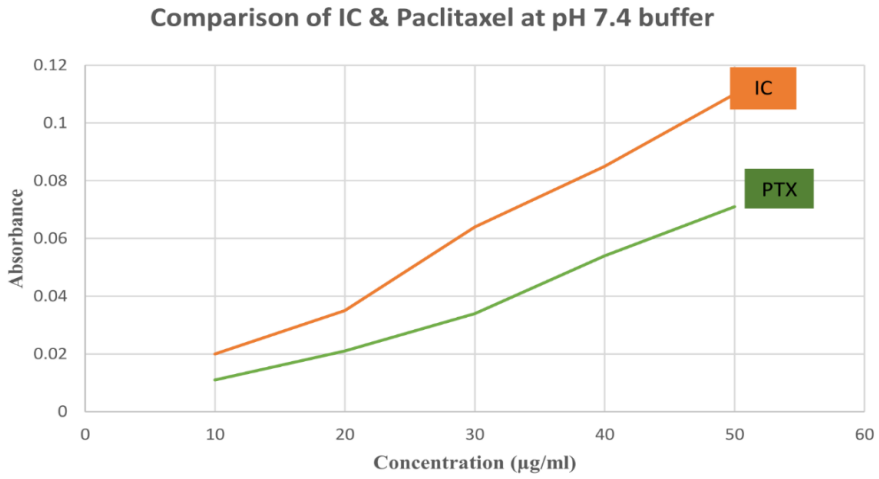

Fig. 12. Apparent aqueous solubility of pure PTX and the PTX–C6A Inclusion complex at pH 7.4, determined by UV–visible spectrophotometry. Data are presented as mean ± SD (n = 3). Statistical significance was analysed using two-way ANOVA

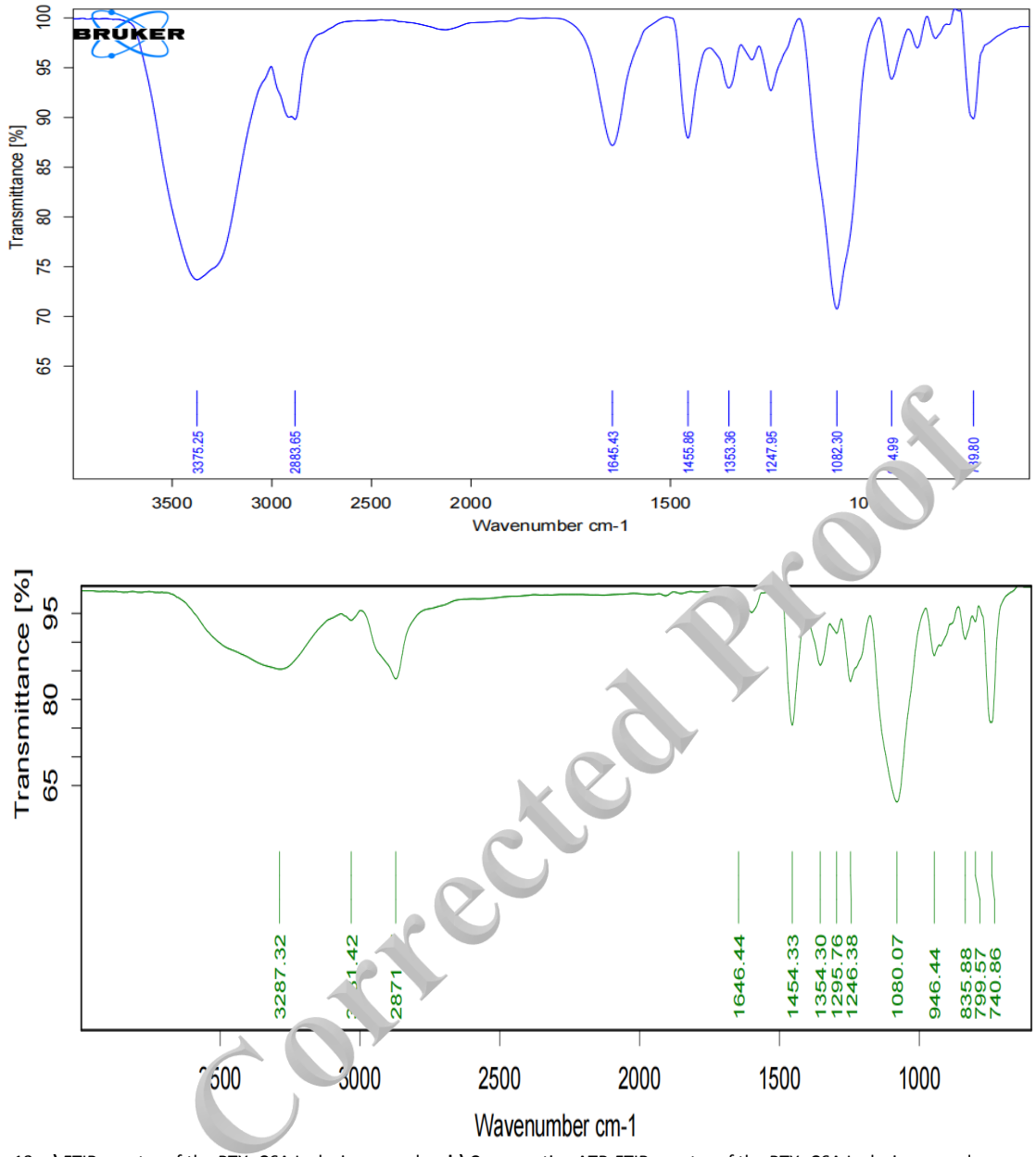

Fig. 13. **a)** FTIR spectra of the PTX–C6A Inclusion complex. **b)** Comparative ATR-FTIR spectra of the PTX–C6A Inclusion complex recorded before and after storage at 4 °C for 12 weeks. No significant changes in the characteristic FTIR absorption bands were observed after storage.

Cytotoxicity assessment by MTT assay

The in vitro cytotoxic effects of Paclitaxel (PTX), Calix[6]arene (C6A), and the PTX–C6A inclusion complex on MIA-Pa-Ca-2 pancreatic cancer cells were assessed using the MTT assay 48 h after treatment (Table 5).

Table 5. Cell viability (%) of MIA-Pa-Ca-2 cells following treatment with PTX, C6A and the PTX–C6A inclusion complex. Data are expressed as mean ± SD (n = 3). Statistical significance was observed between PTX and the PTX–C6A inclusion complex at 5 nM (p = 0.017) and 10 nM (p = 0.0045). No significant differences were observed between C6A and the other treatment groups (p > 0.05)

Formulation	PTX	C6A	IC
0.1 nM	0.509 ± 0.056	0.509 ± 0.056	0.509 ± 0.056
0.25 nM	0.504 ± 0.056	0.507 ± 0.056	0.491 ± 0.055
0.5 nM	0.477 ± 0.051	0.499 ± 0.053	0.480 ± 0.052
1 nM	0.469 ± 0.049	0.492 ± 0.052	0.451 ± 0.045
5 nM	0.313 ± 0.021	0.400 ± 0.032	0.290 ± 0.037
10 nM	0.240 ± 0.018	0.304 ± 0.024	0.236 ± 0.029

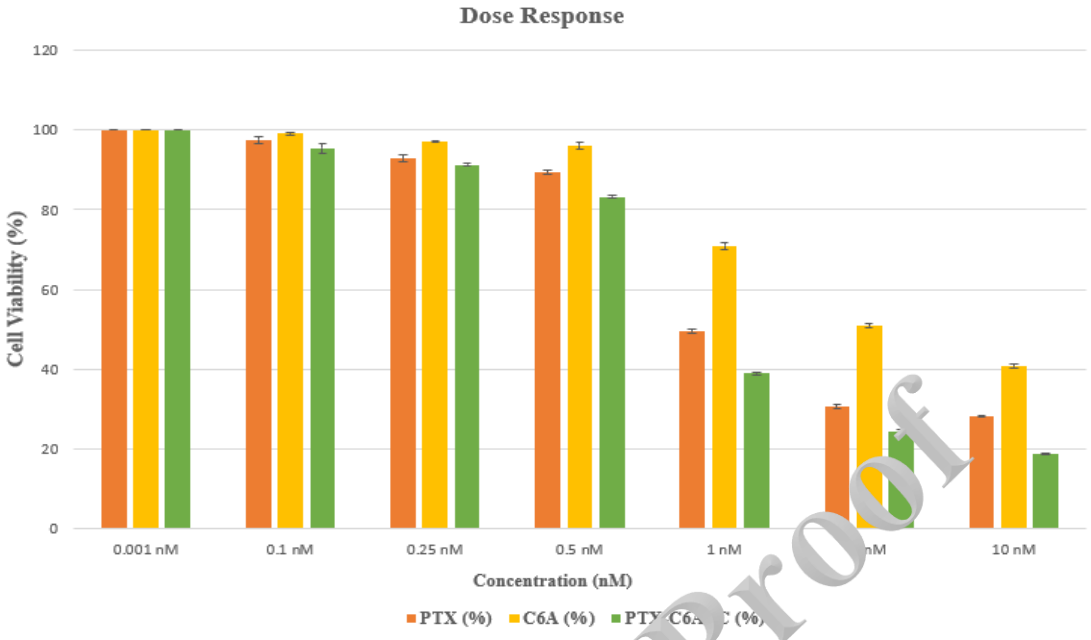

Fig. 14. Cell viability of MIA-Pa-Ca-2 cells following treatment with PTX, C6A, and the PTX–C6A inclusion complex for 48 h. Data are presented as mean ± SD (n = 3), with error bars representing standard deviation.

Cell viability analysis

The cytotoxic responses of PTX, C6A, and the PTX–C6A inclusion complex were investigated over a concentration range of 0.001–10 nM using the MTT assay. As illustrated in Figure 14, all formulations produced a concentration-dependent decline in cell viability. At lower concentrations (0.001–0.25 nM), cell viability remained above 90 % in all treatment groups, indicating negligible cytotoxic effects. Cell viability progressively decreased as the concentration increased, but an antiproliferative response was observed at 1 nM.

Among the various formulations used, the PTX–C6A inclusion complex exhibited the highest in vitro cytotoxic activity at 10 nM concentration. At 1 nM, the cell viability upon treatment with the inclusion complex was about 39 %, whereas the cell viabilities were 49 % for free PTX and 71 % for C6A. At the highest concentration of 10 nM, the cell viability with the inclusion complex was 19 %, whereas the cell viability values were 28 % for PTX and 48 % for C6A alone. The above results suggest that the PTX–C6A inclusion complex exhibited greater antiproliferative activity than PTX alone against MIA-Pa-Ca-2 pancreatic cancer cells (Table 6).

The greater cytotoxic efficiency of the PTX–C6A inclusion complex may be attributed to the improved dispersion and solubilisation of Paclitaxel within the Calix[6]arene molecule, thereby enhancing its availability to cancer cells. On the other hand, Calix[6]arene alone exhibited relatively weak inhibition of cell growth, even at the highest concentration tested, indicating that the enhanced antiproliferative activity was primarily associated with PTX in the inclusion complex.

Determination of IC_{50} Values

The in vitro cytotoxic activity of PTX, C6A and the PTX–C6A inclusion complex was determined in MIA-Pa-ca-2 cells after an exposure of 48 h, using the MTT method to evaluate cell viability. As shown in Figure 12, the applied formulations showed cytotoxic activity, reducing cell viability. A concentration-dependent increase in antiproliferative activity was observed.

Table 6. Cell viability of MIA-Pa-Ca-2 pancreatic cancer cells following treatment with PTX, C6A, and the PTX–C6A Inclusion complex for 48 h.

Concentration (nM)	PTX (%)	C6A (%)	PTX–C6A IC (%)
0.001 nM	100.00 ± 0.00	100.00 ± 0.00	100.00 ± 0.00
0.1 nM	97.57 ± 0.95	99.07 ± 0.47	95.48 ± 1.28
0.25 nM	92.83 ± 0.90	97.12 ± 0.21	91.33 ± 0.49
0.5 nM	89.28 ± 0.54	96.22 ± 0.88	83.25 ± 0.31
1 nM	49.44 ± 0.47	70.93 ± 0.87	38.88 ± 0.46
5 nM	30.64 ± 0.36	50.92 ± 0.67	24.48 ± 0.49
10 nM	28.10 ± 0.13	40.73 ± 0.47	18.84 ± 0.19

Table 7. IC_{50} values obtained from nonlinear regression analysis of the MTT assay

Formulation	IC_{50} (nM)	95 % Confidence Interval (nM)	R^2
Paclitaxel (PTX)	6.705	6.175–7.253	0.9972
Calix[6]arene (C6A)	9.498	8.039–10.91	0.9851
PTX–C6A Inclusion complex	5.641	5.109–6.210	0.9960

The data were analysed using four-parameter logistic regression, which showed a good fit to the experimental data, with R^2 values ranging from 0.9851 to 0.9972. The inclusion complex (IC) showed the highest cytotoxic activity among the tested formulations (IC_{50} = 5.64 nM). This was followed by free PTX (IC_{50} = 6.71 nM) and C6A (IC_{50} = 9.50 nM) (Table 7). The PTX–C6A inclusion complex showed improved antiproliferative activity compared with free PTX and C6A.

The experimental IC_{50} values indicated that the potency of PTX in the form of its complex was 1.19 times higher than that of free PTX and 1.68 times greater than that of C6A. Collectively, these findings suggest that the complexation of Paclitaxel with Calix[6]arene contributes to enhanced in vitro antiproliferative activity against MIA-Pa-Ca-2 pancreatic cancer cells.

The IC_{50} values were determined using four-parameter logistic nonlinear regression analysis of the concentration-response data in GraphPad Prism 11.0.2 (Figure 15). The reported values represent the best fit estimates obtained from three independent experiments.

DISCUSSION

Paclitaxel (PTX) is a major drug in the chemotherapy of many cancers, including pancreatic ductal adenocarcinoma (PDAC). However, its clinical use is limited by poor water solubility and the use of Cremophor EL as a solubilising agent, which is associated with hypersensitivity reactions and peripheral neurotoxicity (38). Since the use of Cremophor can lead to various side effects, the development of a Cremophor-free PTX formulation has become an important subject for investigation. In this study, a PTX–C6A inclusion complex was prepared using a simple physical mixing method. The findings suggest that the inclusion complex possesses improved physicochemical properties, greater apparent aqueous solubility, good stability under the investigated storage conditions, and enhanced in vitro antiproliferative activity against MIA-Pa-Ca-2 pancreatic cancer cells. These results provide evidence that Calix[6]arene can be used as an alternative macrocyclic compound for PTX delivery, thus enriching the literature on supramolecular systems based on Calixarene for pancreatic cancer treatment.

The preparation procedure and molar ratio of the host to guest are important factors in the formation of supramolecular complexes. Among the preparation methods investigated, the physical mixing method using a PTX:C6A molar ratio of 3:5 resulted in the highest drug content, suggesting that it was the most suitable method for preparing the PTX–C6A inclusion complex. The controlled stirring conditions may promote host–guest interactions between PTX and Calix[6]arene, thereby facilitating inclusion complex formation. Reversible noncovalent interactions may contribute to the enhanced aqueous solubility of PTX, as demonstrated in peptide-based supramolecular systems.

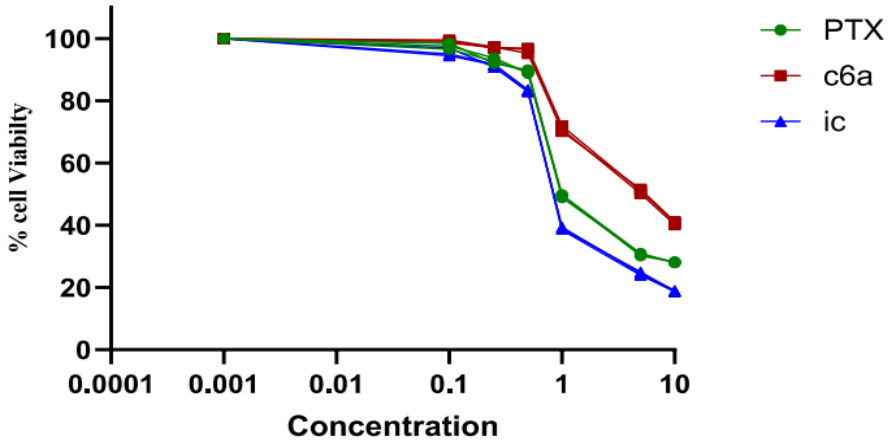

Fig. 15. Dose–response curves of PTX, C6A, and the PTX–C6A Inclusion complex against MIA-Pa-Ca-2 cells, showing the calculated IC_{50} values obtained by nonlinear regression analysis using GraphPad Prism 11.0.2.

Due to the large diterpenoid structure of PTX, full encapsulation in a Calix[6]arene cavity is unlikely. Consequently, for a significantly better drug content, partial PTX inclusion and subsequent stabilisation through multiple noncovalent interactions between PTX and the aromatic cavity of Calix[6]arene is more plausible (39). These are typical features of supramolecular host–guest systems that allow modulation of the physicochemical properties of a drug without changing its chemical structure. The successful realisation of the PTX–C6A inclusion complex indicates that a relatively simple supramolecular strategy can enhance PTX incorporation while altering its chemical structure and can potentially serve as a feasible alternative to sophisticated carrier systems.

Physicochemical characterisation provided complementary evidence supporting the successful formation of the PTX–C6A inclusion complex. The ATR-FTIR spectra retained the characteristic absorption peaks of PTX and C6A, with minimal changes in peak position and bandwidth, indicating that no major chemical structure alteration of PTX occurred. Such results are consistent with the inclusion complex formation by means of reversible noncovalent host–guest interactions, involving hydrophobic interactions, hydrogen bonding, and π–π stacking, without altering the chemical structure of PTX. The lack of noticeable spectral changes upon storage of the samples at 4 °C for 1 weeks demonstrates the stability of the molecular interactions under the studied conditions.

The DSC thermograms and XRD patterns provide complementary evidence of the altered solid-state characteristics following supramolecular complexation. The suppression of the characteristic melting endotherm of PTX together with the marked reduction in crystalline diffraction intensity, indicates partial amorphisation and disruption of the ordered crystal lattice. Unlike complete amorphisation, which may compromise physical stability, partial amorphisation can improve dissolution while retaining acceptable solid-state stability (40). The observed reduction in crystallinity is likely to have contributed to the enhanced apparent aqueous solubility of PTX by increasing molecular mobility and facilitating interactions with the dissolution medium. Similar effects on crystallinity have also been demonstrated for PTX supramolecular systems using cyclodextrin carriers, which correlate with increased dissolution and biological efficacy.

FESEM morphological examination showed that there was a change in the form of PTX from the irregular crystalline form to more consistent particles in the PTX–C6A inclusion complex. The results obtained through morphological examination support the structural modifications shown in DSC and XRD analyses. Additionally, EDS revealed that the elemental composition and homogenous distribution of C, O, and N in the formulation were as expected. This suggests a successful and homogeneous elemental distribution of the PTX–C6A inclusion complex with no elemental impurities detected. Overall, the results show that the optimised formulation constitutes a stable supramolecular system based on molecular recognition phenomena.

Structural modifications caused by supramolecular complexation were evident from the apparent aqueous solubility. The PTX–C6A inclusion complex showed higher aqueous solubility than free PTX under physiological (pH 7.4) and mildly acidic (pH 6.8) conditions. Notably, the enhancement in solubility is more pronounced at pH 6.8. This phenomenon could be due to favourable guest–host interactions, a reduction in crystallinity, and better molecular distribution of PTX within the supramolecular structure. Although no direct studies have been conducted on the molecular mechanisms underlying this pH-dependent behaviour, the observed improvement in apparent aqueous solubility at pH 6.8 suggests that the PTX–C6A inclusion complex may be a promising candidate for further pharmaceutical development in the tumour microenvironment. There are studies focused on the improvement of PTX solubility using noncovalent interactions between peptides or cyclodextrins, highlighting the significance of guest-host interactions in improving the performance of poorly water-soluble drugs [37].

Moreover, the PTX–C6A inclusion complex was characterised by higher in vitro antiproliferative activity against MIA-Pa-Ca-2 pancreatic cancer cells than free PTX, which may be related to improved physicochemical properties. Although all three forms caused a concentration-dependent viability decrease, the inclusion complex had the highest growth inhibition rate and lowest IC_{50}. As no major chemical structural alteration of the Paclitaxel was observed, the increased antiproliferative activity may be related to improved pharmaceutical properties rather than a change in the intrinsic pharmacology of PTX. It is believed that increased apparent solubility and decreased crystallinity may increase the amount of dissolved PTX available to interact with the tumour cells during the 48 h treatment period, thus increasing drug availability under in vitro conditions. The good consistency of the nonlinear regression model is another piece of

evidence of the reliability of the calculated IC_{50} values and the good R^2 of the concentration–response curves obtained. Such improvements in the biological properties of PTX after supramolecular complexation have been described earlier for PTX–Cyclodextrin complexes. Increased drug dissolution and availability result in increased antiproliferative activity of PTX without changing its chemical structure.

Though an enhancement in the antiproliferative activity of the PTX–C6A inclusion complex could be attributed to the improved physicochemical properties of the drug, the specific mechanisms at the cellular level have yet to be elucidated. The current research was not designed to test the cellular uptake of inclusion complexes, intracellular drug transport, microtubule stabilisation, cell cycle arrest, or any form of apoptosis induction. As such, no conclusions regarding the underlying molecular mechanisms of the enhanced biological activity can be made at this stage. Notably, Calix[6]arene itself displayed some degree of antiproliferative activity, implying that apart from acting as a supramolecular carrier, the macrocycle itself exhibits some biological activity. In fact, there are several reports on the modulation of receptor tyrosine kinase signalling, induction of endoplasmic reticulum stress, and activation of autophagy via selected derivatives of calixarenes, which contribute to their antiproliferative effects. However, these mechanisms have never been associated with the parent Calix[6]arene used in this study. Hence, the enhanced biological activity of the PTX–C6A inclusion complex could be attributed to the improved pharmaceutical properties of PTX, as opposed to the cytotoxicity of the carrier itself.

The present results are consistent with prior reports showing that supramolecular complexation is a viable approach for improving Paclitaxel pharmaceutical performance without chemically altering its Paclitaxel molecular structure. Most reported PTX delivery systems employ β-cyclodextrin-based carriers because of their well-established ability to enhance aqueous solubility and dissolution via host–guest interactions. For example, Liu *et al.* developed bridged bis(β-cyclodextrin) inclusion complexes that improved the solubility and antitumour activity of PTX. In contrast, Shah reported enhanced aqueous solubility and cellular uptake using β-cyclodextrin derivatives [14]. Similarly, Zarrabi and Vossoughi demonstrated improved PTX complexation using β-cyclodextrin-grafted polymeric carriers [18], while Ye *et al.* incorporated PTX–cyclodextrin inclusion complexes into chitosan nanoparticles to further improve drug delivery and pharmacokinetic performance [16]. Collectively, these studies demonstrate that host–guest complexation is an effective strategy for overcoming the poor aqueous solubility of PTX.

In contrast to these studies, which mostly involve cyclodextrins as host molecules, studies involving Calix[6]arene as a supramolecular host for PTX are few. This present study expands current knowledge of calixarenes-based drug delivery by demonstrating that a PTX–C6A inclusion complex formulated through a relatively simple physical mixture can achieve better drug loading, alter the properties of PTX in its solid-state form, increase its apparent solubility in water, and increase its in vitro antiproliferative activity towards MIA-PaCa-2 pancreatic cancer cells. Unlike some previous formulations of PTX, which involve polymer and nanomaterial-based formulations, the present approach uses a simpler strategy based solely on supramolecular complexation without the use of Cremophor EL. However, one should be careful in comparing results from these different studies because of the possibility of these differences being explained by variations in the formulation design and preparation methodologies. Nonetheless, although there are some limitations, Calix[6]arene is established as a viable host molecule for making non-Cremophor formulations of PTX.

Despite the promising evidence for the PTX–C6A inclusion complex, several limitations should be discussed. This study focused solely on physicochemical characterisation and in vitro evaluation using only a pancreatic cancer cell line. Cellular uptake, signalling related to the apoptosis death pathway, pharmacokinetic properties, as well as biodistribution and in vivo therapeutic efficacy were not examined in this study. Moreover, although C6A itself exhibited antiproliferative activity, the mechanism underlying this effect remains unclear and requires further investigation. Therefore, future studies must assess both the intracellular fate of the inclusion complex and the molecular mechanisms underlying its anticancer action, pharmacokinetic parameters, and therapeutic efficiency in suitable animal tumour models for pancreatic cancer to confirm its translational relevance.

Overall, it can be concluded that supramolecular complexation with Calix[6]arene is a viable method to improve the physicochemical properties, apparent solubility, and in vitro

antiproliferative activity of Paclitaxel, without the use of Cremophor EL. In particular, the increased efficiency of drug incorporation into the matrix, solid-state properties, aqueous solubility, stability and antiproliferative effect of the compound in vitro show that Calix[6]arene is an appropriate macrocyclic carrier or host for PTX transport. Although further comprehensive studies are required before any potential clinical applications, these findings provide a basis for further development of simple Cremophor-free supramolecular formulations.

CONCLUSIONS

This study describes an optimised physical mixing method for preparing a Cremophor-free PTX–C6A inclusion complex at a PTX:C6A molar ratio of 3:5, offering a simple supramolecular approach to improve the pharmaceutical performance of Paclitaxel. Extensive physicochemical characterisation by ATR-FTIR, DSC, XRD, FESEM, EDS and HPLC provided complementary evidence supporting host–guest complex formation, partial amorphisation and successful PTX incorporation into the PTX–C6A inclusion complex. The PTX–C6A inclusion complex showed a significantly higher apparent aqueous solubility than free PTX both under physiological and at tumour-mimicking conditions, acceptable physicochemical stability during the storage period, and higher antiproliferative activity in vitro against MIA-Pa-Ca-2 pancreatic cancer cells. Overall, these findings support the potential of Calix[6]arene as a supramolecular host for future Cremophor-free PTX formulations, supporting the enhanced pharmaceutical performance of poorly water-soluble anticancer agents. These findings provide a basis for further investigation of calixarene-based supramolecular drug delivery systems for hydrophobic anticancer drugs. Nevertheless, there is a need for additional research on how these PTX–C6A inclusion complexes are internalised by cells, their mechanism of action and pharmacokinetic profiles.

AUTHORS CONTRIBUTION

J. S.: Conceptualisation, methodology, formulation development, experimental investigation, HPLC analysis, physicochemical characterisation, apparent solubility studies, stability studies, cytotoxicity studies, data curation, formal analysis, and writing—original draft. **B. G.**: Supervision, methodology, interpretation of results, critical review of the manuscript, and writing-review and editing. **S. K. G.**: Supervision, project administration, scientific guidance, interpretation of results, and writing-review and editing.

FUNDING

The authors did not receive any support from any organisation for this work. This research was entirely self-funded by the authors.

CONFLICT OF INTEREST

The authors declare that they have no competing financial interests or personal relationships that could influence the work reported in this study.

ETHICAL APPROVAL

This study did not include any preclinical or clinical studies.

ARTIFICIAL INTELLIGENCE (AI) DECLARATION

All scientific interpretations, analyses, and conclusions were independently verified by the authors. The author declares that Claude AI was used to generate a graphical abstract and was modified using Canva AI.

INFORMED CONSENT

Not applicable.

ACKNOWLEDGEMENT

I am thankful to my colleagues, family, SRIP, and VU for their support, guidance, and resources. Furthermore, I sincerely acknowledge Dr. Bina Gidwani for her valuable guidance, constant encouragement, and insightful suggestions throughout this research work. I also express my gratitude to Dr. Sanjay Kumar Gupta for his continuous support, technical assistance, and constructive inputs during the study.

REFERENCES

1. Bayat M, Nahand JS. Battlegrounds of treatment resistance: decoding the tumour microenvironment. Naunyn Schmiedebergs Arch Pharmacol. 2025;398(9):11179–11197.
2. Hidalgo M. Pancreatic cancer. N Engl J Med. 2010;362(17):1605–1617.
3. Igarashi H, Ito T, Hisano T, Fujimori N, Niina Y, Yasuda M, et al. Paclitaxel-based chemotherapy for advanced pancreatic cancer after gemcitabine-based therapy failure: a case series of 5 patients. Case Rep Oncol. 2011;4(3):534–541.
4. Ejeta BM, Das MK, Das S. Recent advances in Paclitaxel drug delivery: challenges, innovations, and future directions. J Angiother. 2024;8(8):1–13.
5. Muley A, Navale A, Gupta R, Tekade RK. Nano-Paclitaxel: unlocking potential and redefining cancer chemotherapy. ACS Omega. 2025;10(27):28670–28690.
6. Suh MS, Patil SM, Kozak D, Pang E, Choi S, Jiang X, et al. An NMR protocol for in vitro Paclitaxel release from an albumin-bound nanoparticle formulation. AAPS Pharm Sci Tech. 2020;21(5):136.
7. Chen Q, Yang Z, Liu H, Man J, Oladejo AO, Ibrahim S, et al. Novel drug delivery systems: an important direction for drug innovation research and development. Pharmaceutics. 2024;16(5):674.
8. Galindo-García U, Torres LA. Crystal structure at the origin of the thermal stability and large enthalpy of

fusion and sublimation values of calixarenes. Cryst Growth Des. 2020;20(2):1302–1310.
9. Barbera L, Gattuso G, Kohnke FH, Notti A, Pappalardo S, Parisi MF, et al. Self-assembly of amphiphilic anionic calix[4]arenes and encapsulation of poorly soluble naproxen and flurbiprofen. Org Biomol Chem. 2015;13(23):6468–6473.
10. Español ES, Villamil MM. Calixarenes: generalities and their role in improving the solubility, biocompatibility, stability, bioavailability, detection, and transport of biomolecules. Biomolecules. 2019;9(3):90.
11. Geng WC, Jiang ZT, Chen SL, Guo DS. Supramolecular interaction in the action of drug delivery systems. Chem Sci. 2024;15(21):7811–7823.
12. Pelizzaro-Rocha KJ, Jesus MB, Ruela-de-Sousa RR, Nakamura CV, Reis FS, de Fátima A, et al. Calix [6] arene bypasses human pancreatic cancer aggressiveness: downregulation of receptor tyrosine kinases and induction of cell death by reticulum stress and autophagy. Biochim Biophys Acta Mol Cell Res. 2013;1833(12):2856–2865.
13. Liu Y, You CC, Zhang HY, Zhao YL. Inclusion complexation and solubilisation of Paclitaxel by bridged bis(β-cyclodextrins) containing a tetraethylenepentaamino spacer. J Med Chem. 2003;46(22):4634–4637.
14. Liu Y, Chen GS, Chen Y, Cao DX, Ge ZQ, Yuan YJ. Inclusion complexes of Paclitaxel and oligo(ethylenediamino)-bridged bis(β-cyclodextrins): solubilisation and antitumour activity. Bioorg Med Chem. 2004;12(22):5767–5775.
15. Choi SG, Lee SE, Kang BS, Ng CL, Davaa E, Park JS. Thermosensitive and mucoadhesive gel-g composites of Paclitaxel/dimethyl-β-cyclodextrin for buccal delivery. PLoS One. 2014; 9(10): 109090.
16. Ye Y, Wang Y, Lou KY, Chen YZ, Chen R, Gao F. Preparation, characterization, and pharmacokinetic studies of chitosan nanoparticles loaded with Paclitaxel/dimethyl-β-cyclodextrin inclusion complexes. Int J Nanomedicine. 2015; 10: 4309–4319.
17. Shah M, Shah V, Ghosh A, Zhang Z, Minko T. Molecular inclusion complexes of β-cyclodextrin derivatives enhance aqueous solubility and cellular internalization of Paclitaxel: preformulation and in vitro assessments. J Pharm Pharmacol (Los Angel). 2015;2(2):8.
18. Zarrabi A, Vossoughi M. Paclitaxel/β-CD-g-PG inclusion complex: an insight into complexation thermodynamics and guest solubility. J Mol Liq. 2015; 208: 145–150.
19. Song X, Wen Y, Zhu JL, Zhao F, Zhang ZX, Li J. Thermoresponsive delivery of Paclitaxel by β-cyclodextrin-based poly(N-isopropylacrylamide) star polymer via inclusion complexation. Biomacromolecules. 2016;17(12):3957–3963.
20. Bhatt P, Lalani R, Vhora I, Patil S, Amrutiya J, Misra A, et al. Liposomes encapsulating native and cyclodextrin-enclosed Paclitaxel: enhanced loading efficiency and its pharmacokinetic evaluation. Int J Pharm. 2018;536(1):95–107.
21. Varan G, Benito JM, Ortiz Mellet C, Bilensoy E. Cellular interaction and tumoural penetration properties of Paclitaxel-loaded amphiphilic cyclodextrin nanoparticles for breast cancer treatment in 2D and 3D in vitro tumour models. Nanomaterials (Basel). 2018;8(2):67.
22. Show S, Dutta D, Nongthomba U, Prasad AJM. Effective Paclitaxel: β-cyclodextrin-based formulation boosts in vitro anti-tumour potential and lowers toxicity in zebrafish. Toxicol Res (Oxf). 2024; 13(5):tfae150.
23. Mohandoss S, Velu KS, Wahab R, Ahmad N, Dhanasekaran K, Kumarappan A. β-Cyclodextrin inclusion complex as a potent delivery system for Paclitaxel against triple-negative human breast cancer. J Nanopart Res. 2025; 27: 229.
24. Kim TY, Kim DW, Chung JY, Shin SG, Kim SC, Heo DS, et al. Phase I and pharmacokinetic study of Genexol-PM, a Cremophor-free polymeric micelle-formulated Paclitaxel, in patients with advanced malignancies. Clin Cancer Res. 2004; 10(11):3708–3716.
25. da Silva Júnior WF, de Oliveira Pinheiro JG, Moreira CDL, de Souza FJJ, de Lima AAN. Alternative technologies to improve solubility and stability of poorly water-soluble drugs. In: Grumezescu AM, editor. Multifunctional systems for combined delivery, biosensing and diagnostics. Amsterdam: Elsevier; 2017; 281–305.
26. Cid-Samamed A, Rakmai J, Mejuto JC, Simal-Gandara J, Astray G. Cyclodextrin inclusion complexes: preparation methods, analytical techniques and food industry applications. Food Chem. 2022; 384: 132467.
27. Budurova D, Momekova D, Momekov G, Shestakova P, Penchev H, Rangelov S. PEG-modified tert-octylcalix[8]arenes as drug delivery nanocarriers of silibinin. Pharmaceutics. 2021;13(12):2025.
28. Meenach SA, Anderson KW, Hilt JZ, McGarry RC, Mansour HM. Characterization and aerosol dispersion performance of advanced spray-dried chemotherapeutic PEGylated phospholipid particles for dry powder inhalation delivery in lung cancer. Eur J Pharm Sci. 2013;49(4):699–711.
29. Bloxham JC, Hogge J, Giles NF, Knotts TA IV, Wilding WV. Modulated differential scanning calorimetry measurements of 27 compounds. J Chem Eng Data. 2021;66(7):2773–2782.
30. Gang C. A doping method for quantitative X-ray diffraction phase analysis of samples containing amorphous material. Acta Phys Sin. 1998;47(7):1143–1149.
31. Wang Y, Wang D, Fu Q, Liu D, Ma Y, Racette K, et al. Shape-controlled Paclitaxel nanoparticles with multiple morphologies: rod-shaped, worm-like, spherical, and fingerprint-like. Mol Pharm. 2014;11(10):3766–3771.
32. Rathi M, Ahrenkiel P, Carapella J, Wanlass MW. A standards-based method to determine elemental compositions using energy dispersive X-ray spectrometry for compound semiconductors. Microsc Microanal. 2012;18(Suppl 2):1046–1047.
33. Badea I, Ciutaru D, Lazar L, Nicolescu D, Tudose A. Rapid HPLC method for the determination of

Paclitaxel in pharmaceutical formulations without separation. J Pharm Biomed Anal. 2004;34(3):501–507.
34. Varma MV, Gardner I, Steyn SJ, Nkansah P, Rotter CJ, Whitney-Pickett C, et al. pH-dependent solubility and permeability criteria for BCS classification of ionizable drugs. Mol Pharm. 2012;9(5):1199–1212.
35. Miloudi L, Bonnier F, Barreau K, Bertrand D, Perse X, Yvergnaux F, et al. ATR-IR coupled to partial least squares regression (PLSR) for monitoring an encapsulated active molecule in complex semi-solid formulations. Analyst. 2018;143(10):2377–2389.
36. Bendale Y, Bendale V, Paul S. Evaluation of cytotoxic activity of platinum nanoparticles against normal and cancer cells and its anticancer potential through induction of apoptosis. Integr Med Res. 2017;6(2):141–148.
37. Shekhawat KS, Bhatia P, Bhatnagar K, Shandilay S, Chaudhary S. Roadmap to cytotoxicity: exploring assays and mechanisms. Assay Drug Dev Technol. 2025;23(5):217–236.
38. Gelderblom H, Verweij J, Nooter K, Sparreboom A. Cremophor EL: the drawbacks and advantages of vehicle selection for drug formulation. Eur J Cancer. 2001;37(13):1590–1598.
39. Liu W, Guo T, Ge JW, Li HY, Xu XJ, Sun LX, et al. An oligopeptide improves the solubility of Paclitaxel by non-covalent interaction. Acta Pharm Sin. 2012;47(7):947–952.
40. Hancock BC, Zografi G. Characteristics and significance of the amorphous state in pharmaceutical systems. J Pharm Sci. 1997;86(1):1–12.